

# The reactions $pp \rightarrow p\Lambda K^+$ and $pp \rightarrow p\Sigma^0 K^+$ near their thresholds

A. Gasparian<sup>a,b</sup>, J. Haidenbauer<sup>a</sup>, C. Hanhart<sup>c</sup>, L. Kondratyuk<sup>b</sup>,  
and J. Speth<sup>a</sup>

<sup>a</sup>Institut für Kernphysik, Forschungszentrum Jülich GmbH,  
D-52425 Jülich, Germany

<sup>b</sup>Institute of Theoretical and Experimental Physics,  
117259, B.Chermushkinskaya 25, Moscow, Russia

<sup>c</sup>Nuclear Theory Group and INT, Dept. of Physics, University of Washington,  
Seattle, WA 98195-1560, USA

---

## Abstract

The reactions  $pp \rightarrow p\Lambda K^+$  and  $pp \rightarrow p\Sigma^0 K^+$  are studied near their thresholds. The strangeness production process is described by the  $\pi$ - and  $K$  exchange mechanisms. Effects from the final state interaction in the hyperon-nucleon system are taken into account rigorously. The  $\Lambda$  production turns out to be dominated by  $K$  exchange whereas  $K$ - as well as  $\pi$  exchange play an important role for the  $\Sigma^0$  case. It is shown that the experimentally observed strong suppression of  $\Sigma^0$  production compared to  $\Lambda$  production at the same excess energy can be explained by a destructive interference between  $\pi$  and  $K$  exchange in the reaction  $pp \rightarrow p\Sigma^0 K^+$ . Implications of such an interference on the reaction  $pp \rightarrow n\Sigma^+ K^+$  are pointed out.

---

Recently the total cross sections for the reactions  $pp \rightarrow p\Lambda K^+$  and  $pp \rightarrow p\Sigma^0 K^+$  were measured for the first time in the threshold region [1–3]. Certainly the most interesting aspect of these new data is the observed strong suppression of the  $\Sigma^0$  production in comparison to the  $\Lambda$  channel: at the same excess energy the cross section for the  $\Sigma^0$  production is about a factor of 25 smaller than the one for the  $\Lambda$  production [3]. This is indeed rather surprising, specifically because data at higher energies [4,5] indicate that the cross section for  $\Lambda$  production exceeds the one for  $\Sigma^0$  production only by a factor of around 2.5.

In principle, this strong suppression of the  $\Sigma^0$  production compared to the  $\Lambda$

case can be understood if one assumes that the hyperon production is solely due to the  $K$ -exchange diagram, depicted in Fig. 1(a). In this case the same elementary ( $K^+p$ ) re-scattering amplitude enters in the two reactions. Therefore the ratio  $\sigma_\Lambda/\sigma_{\Sigma^0} := \sigma_{pp \rightarrow p\Lambda K^+}/\sigma_{pp \rightarrow p\Sigma^0 K^+}$  will be given essentially by the ratio of the coupling constants at the vertices from which the  $K$  meson emerges, i. e. by  $g_{\Lambda NK}^2/g_{\Sigma NK}^2$ . These coupling constants are not very well known experimentally. However, they can be inferred from SU(3) flavour symmetry - a symmetry which, so far, has been rather successfully employed in investigations of reactions involving hyperons. Specifically according to SU(6) this ratio is 27 [6], a value which coincides almost exactly with the experimental cross section ratio.

None-the-less, already a simple estimation of the elementary scattering processes ( $K^+p \rightarrow K^+p$  and  $\pi^0 p \rightarrow K^+\Lambda, K^+\Sigma^0$ , respectively) based on experimental amplitudes reveals that the contribution of the  $\pi$ -exchange diagram (Fig. 1(b)) to hyperon production should be not negligible, cf. Ref. [3]. Strong evidence for the relevance of  $\pi$ -exchange comes also from more detailed model calculations [7–12]. (It should be said, however, that most of these studies focus on data at rather large excess energies or look at the  $\Lambda$  channel only.) Indeed the  $\Lambda/\Sigma^0$  production ratio estimated in Ref. [3], considering  $K$ - as well as  $\pi$  exchange, is roughly 3.6, i.e. about a factor of 8 below the measurement.

Because of this situation another explanation for the observed suppression of the  $\Sigma^0$  production was suggested in Ref. [3], namely effects from the strong  $\Sigma N$  final state interaction (FSI) leading to a  $\Sigma N \rightarrow \Lambda N$  conversion. (Note that such FSI effects have been ignored in the above discussion altogether!) Evidence suggesting this conversion hypothesis can be readily found in the literature. E.g., the predictions of modern meson-theoretical models of the hyperon-nucleon  $YN$  interaction for the  $\Lambda N$  cross section show a large cusp structure at the  $\Sigma N$  threshold, which arises from the strong coupling between the  $\Lambda N$  and  $\Sigma N$  channels in those models [13,14]. Inclusive measurements of  $K^+$  production in the reaction  $pp \rightarrow K^+X$  at 2.3 GeV show a significant enhancement near the  $\Sigma N$  threshold [15]. Finally, data on the reaction  $K^-d \rightarrow \pi^-\Lambda p$  show a sharp peak at an effective mass of  $m_{\Lambda p} \approx 2130 \text{ MeV}/c^2$ , i.e. at the  $\Sigma N$  threshold [16]. (Cf. also corresponding theoretical investigations in Refs. [17,18].) Thus, it is obvious that there is a strong enhancement of the  $\Lambda$  counting rate in those reactions. However, it is much less clear whether this enhancement is indeed due to produced “real”  $\Sigma$ ’s being converted into  $\Lambda$ ’s in the FSI so that the number of experimentally observed  $\Sigma$ ’s in any exclusive measurement will be greatly reduced.

In the present paper we want to study the  $\Lambda$  and  $\Sigma^0$  production cross section in  $pp$  collisions near threshold. Thereby our emphasis will be on a careful treatment of the FSI. Specifically we want to investigate in detail possible effects from the  $\Sigma \leftrightarrow \Lambda$  conversion. In order to have a solid basis for our

study we employ microscopic  $YN$  interaction models from the Jülich [13] and Nijmegen [14] groups. The Jülich  $YN$  model is derived in the meson-exchange picture and has been constructed according to the same guidelines as those used in the Bonn  $NN$  potential [19]. The model is given in momentum space and contains the full nonlocal structure resulting from the relativistic meson exchange framework. The parameters at the  $NN$  vertices (coupling constants and cutoff masses in the form factors) are taken from the Bonn potential. The coupling constants at the strange vertices are determined from  $SU(6)$  symmetry relations. The only free parameters in this model are the cut-off masses of the form factors at the strange vertices - which are determined by a fit to the empirical hyperon-nucleon data. The model describes existing  $\Lambda N$  and  $\Sigma N$  observables reasonably well as can be seen in Ref. [13].

Besides the Jülich model we will also employ potential models provided by the Nijmegen group [14]. This will allow us to investigate the model dependence of our results. The Nijmegen NSC97 potentials provide a comparably good description of the available  $YN$  data. However, there are quite significant differences in the dynamical input of the Nijmegen models and that of the Jülich group as discussed, e.g., in Ref. [20]. Thus, it is possible that these differences play a role in the present analysis, specifically because in the associated strangeness production it will be mostly the off-shell properties of these  $YN$  models that enter into the calculation.

We treat the associated strangeness production in the standard distorted wave Born approximation. Thus, the production amplitude  $M$  is obtained from the formal equation

$$M = A + AG_0 T_{YN} , \quad (1)$$

where  $A$  is the elementary production process ( $\pi$ - and/or  $K$  exchange, Fig. 1),  $T_{YN}$  the interaction in the final state, and  $G_0$  the free  $YN$  propagator. Note that the second term on the right-hand side involves, in fact, a sum over the (coupled)  $\Lambda N$  and  $\Sigma N$  states. This can be seen from the graphic representation of Eq. 1 in Fig. 2 (for the case of  $\Lambda$  production).

Following standard rules [21] one gets the following expression for the anti-symmetrized Born amplitudes,

$$A_K^{\mu_1\mu_2\mu_3\mu_4}(\vec{p}_1, \vec{p}_2; \vec{p}_3, \vec{p}_4) = F_K(\vec{p}_3 - \vec{p}_1) \Gamma_{NYK}^{\mu_1\mu_3} \frac{2\omega_K}{k_K^2 - m_K^2} T_{KN}^{\mu_2\mu_4} - (\vec{p}_1 \leftrightarrow \vec{p}_2, \mu_1 \leftrightarrow \mu_2) \quad (2)$$

$$A_\pi^{\mu_1\mu_2\mu_3\mu_4}(\vec{p}_1, \vec{p}_2; \vec{p}_3, \vec{p}_4) = F_\pi(\vec{p}_4 - \vec{p}_1) \Gamma_{NN\pi}^{\mu_1\mu_4} \frac{2\omega_\pi}{k_\pi^2 - m_\pi^2} T_{\pi N \rightarrow KY}^{\mu_2\mu_3} - (\vec{p}_1 \leftrightarrow \vec{p}_2, \mu_1 \leftrightarrow \mu_2) \quad (3)$$

where the  $\mu_i$  ( $\vec{p}_i$ ) are the spin projections (momenta) of the baryons,  $k_K$  and  $k_\pi$  are the four momenta of the exchanged kaon and pion, and  $\omega_K = \sqrt{(\vec{p}_3 - \vec{p}_1)^2 + m_K^2}$  and  $\omega_\pi = \sqrt{(\vec{p}_4 - \vec{p}_1)^2 + m_\pi^2}$  are their energies.  $T_{KN}$  and  $T_{\pi N \rightarrow KY}$  are the amplitudes of the corresponding elementary reactions.  $\Gamma_{NYK}$  and  $\Gamma_{NN\pi}$  are vertex functions for the corresponding baryon-baryon-meson vertices,

$$\Gamma^{\mu_i \mu_j} = i \frac{f_{B_i B_j M}}{m_M} \frac{1}{(2\pi)^{3/2}} \frac{1}{\sqrt{2\omega_M}} N_i N_j \times \chi_{\mu_j}^\dagger \vec{\sigma} \cdot \left[ \vec{k}_M - \omega_M \left( \frac{\vec{p}_i}{\epsilon_{p_i}} + \frac{\vec{p}_j}{\epsilon_{p_j}} \right) + \left( \frac{\vec{p}_i^2 \vec{p}_j - \vec{p}_j^2 \vec{p}_i}{\epsilon_{p_i} \epsilon_{p_j}} \right) \right] \chi_{\mu_i} \quad (4)$$

where  $\epsilon_{p_i} = E_{p_i} + m_i$  and  $N_i = \sqrt{\frac{\epsilon_{p_i}}{2E_{p_i}}}$ , and  $F_K$  and  $F_\pi$  are form factors which are assumed to be of monopole type, i.e.  $F_M(\vec{k}) = (\Lambda_M^2 - m_M^2)/(\Lambda_M^2 + \vec{k}^2)$ .

The total cross section is obtained from

$$\sigma = \frac{1}{4v} \sum_{\mu_i, \mu_f} \int d^3 p_3 d^3 p_4 d^3 p_{K^+} (2\pi)^4 \delta^{(4)}(P_f - P_i) |M_{i \rightarrow f}|^2 \quad (5)$$

where  $p_K^+$  is the momentum of the produced kaon and  $v$  is the relative velocity of the two initial protons.

The vertex parameters employed in the present study are compiled in Table 1. For the calculation with the Jülich  $YN$  interaction we take the same values that were used in this model. In case of the Nijmegen model we take over only their coupling constants but not their vertex form factors. For simplicity reasons we use here also a monopole form - but with a uniform cutoff parameter of  $\Lambda = 1.3$  GeV.

The elementary amplitudes  $T_{KN}$  and  $T_{\pi N \rightarrow KY}$  can be taken from microscopic models of  $KN$  scattering [22] and of the reaction  $\pi N \rightarrow K\Lambda, K\Sigma$  [23] that were developed by our group. However, since in the present more exploratory study we would like to focus mainly on the FSI effects we will restrict ourselves to a simplified treatment of the production amplitude. Thus, instead of the full (off-shell)  $KN$  and  $\pi N \rightarrow KY$  transition amplitudes we use the scattering length and on-shell threshold amplitudes of those reactions. The off-shell extrapolation of the amplitudes is done by multiplying those quantities with the same form factor that is used at the vertex where the exchanged meson is emitted. Furthermore we take into account only s waves. For the  $KN$  s-wave scattering lengths we employ the values  $a^0 = -0.038$  fm and  $a^1 = -0.304$  fm (for the isospin 0 and 1 states) resulting from our  $KN$  model [22], which are in good agreement with experimental information [24]. For the  $\pi N \rightarrow KY$  amplitudes we use  $f_{\pi^0 p \rightarrow K^+ \Lambda} = (-0.06 + i0.48) \times 10^{-1}$  fm,  $f_{\pi^0 p \rightarrow K^+ \Sigma^0} =$

$(0.45 - i0.35) \times 10^{-1} fm$ , and  $f_{\pi^+p \rightarrow K^+\Sigma^+} = (-0.11 + i0.21) \times 10^{-1} fm$ . The value for the first reaction yields  $|f_{\pi^0p \rightarrow K^+\Lambda}|^2 = 29 \mu b/sr$  which is comparable to the number deduced by Fäldt and Wilkin [25] from  $\pi^-p$  data [26]. For the other reactions we get  $|f_{\pi^0p \rightarrow K^+\Sigma^0}|^2 = 33 \mu b/sr$  and  $|f_{\pi^+p \rightarrow K^+\Sigma^+}|^2 = 5.7 \mu b/sr$ . From those scattering amplitudes the T-matrices are obtained via the relation

$$f_{MB \rightarrow M'B'} = -4\pi^2 \frac{\sqrt{E_B \omega_M E_{B'} \omega_{M'}}}{E_B + \omega_M} T_{MB \rightarrow M'B'} \quad (6)$$

using the threshold kinematics.

Since we will concentrate on energies very close to the thresholds we consider only the lowest partial waves in the outgoing channels; the  $\Lambda p$  and  $\Sigma^0 p$  system can be in an  $^1S_0$  or in a  $^3S_1$  state and the  $K^+$  is assumed to be in an s-wave relative to the  $YN$  state. Angular momentum and parity conservation then tells us that the initial  $pp$  system has to be in the  $^3P_0$  or in the  $^3P_1$  state. Note that the  $^3S_1$  partial wave couples to the  $^3D_1$  and this coupling is taken into account in our calculations.

We do not take into account the initial state interaction (ISI) between the protons. Based on a recent examination of the influence of the ISI for the reaction  $pp \rightarrow pp\eta$  by Batinić et al. [27] we expect that the neglect of the ISI should result in an overestimation of the cross sections by a factor of around 3 in our calculation (cf. also Ref. [28]). But since the thresholds for the  $\Lambda$  and  $\Sigma^0$  production are relatively close together (at  $T_{lab} = 1582$  MeV and at  $T_{lab} = 1796$  MeV) and, moreover, the energy dependence of the  $NN$  interaction is relatively weak in this energy region we expect that the ISI effects are very similar for the two strangeness production channels and therefore should roughly drop out when ratios of the cross sections are taken. Thus, we believe that our model calculation allows a quite reliable estimation of  $\sigma_\Lambda/\sigma_{\Sigma^0}$ . The same is also true for a comparison of the relative magnitude of the pion- and kaon-exchange contributions.

The FSI increases considerably the number of contributing amplitudes as can be seen from the graphs shown in Fig. 2. Besides the Born terms (Fig. 2a,e) there are contributions from the "diagonal" FSI (Fig. 2b,f) and from the transitions with  $p\Sigma^0$  and  $n\Sigma^+$  intermediate states (Fig. 2c,g and d,h, respectively). All these contributions have to be added coherently for the evaluation of the production cross section. In order to investigate the influence of the FSI in detail and to clarify the roles played by the  $\pi$ - and  $K$ -exchange we have also evaluated the contributions of the individual diagrams and compiled them in Tables 2 (for the Jülich model A) and 3 (for the Nijmegen model NSC97f). The analysis is done for the data at the highest available excess energy, i.e. 13.2 MeV for the  $\Lambda$  production and 13.0 MeV for the  $\Sigma^0$  production.

Let us first discuss the  $K$  exchange. The cross section ratio resulting from the Born diagram alone is around 16 for the Jülich model, cf. Table 2. Based on the ratio of the coupling constants (Table 1) one would have expected a value close to 27. However, one has to keep in mind that a much harder form factor is employed at the  $\Sigma NK$  vertex than at the  $\Lambda NK$  vertex (cf. Ref. [13]) which obviously has a strong impact on the actual results. Now we add the amplitude of the "diagonal" FSI which means diagram (b) of Fig. 2 for  $\Lambda$  production and diagrams with  $\Sigma^+ n$  and  $\Sigma^0 p$  intermediate states for  $\Sigma^0$  production. This is the step where a possible conversion effect  $\Sigma N \rightarrow \Lambda N$  should become visible. The employed  $\Sigma N$  t-matrix is the solution of the coupled-channel scattering equation and therefore includes the flux going from the  $\Sigma N$  to the  $\Lambda N$  system. Indeed the consideration of the "diagonal" FSI enhances the cross section of the  $\Lambda$  channel and reduces the one of the  $\Sigma^0$  channel. As a consequence, the resulting cross section ratio becomes significantly larger than the value obtained from the Born term and is even close to the experimental value, cf. Table 2. In the final step we add the diagram where a transition  $\Sigma N \leftrightarrow \Lambda N$  occurs in the FSI (cf. Fig. 2c,d). This leads to further modifications in the cross sections and to a further increase in cross section ratio.

In case of pion exchange the Born diagrams yield a cross section ratio of 0.9. This value is somewhat larger than the estimate presented in Ref. [3] because now the isospin  $\frac{3}{2}$  component of the  $\pi N \rightarrow K\Sigma$  amplitude was taken into account as well. Adding the FSI step by step increases the cross section ratio somewhat, but it remains far below the experiment.

Thus, it's clear that, in principle,  $K$  exchange alone can explain the cross section ratio - especially after inclusion of FSI effects. However, we also see from Table 2 that  $\pi$  exchange definitely yields a significant contribution to the  $\Sigma^0$  channel and therefore it cannot be ignored. Indeed, the two production mechanisms play quite different roles in the two reactions under consideration, cf. Table 2.  $K$  exchange yields by far the dominant contribution for  $pp \rightarrow p\Lambda K^+$ . Here the cross section obtained from  $\pi$  exchange is about an order of magnitude smaller. In case of the reaction  $pp \rightarrow p\Sigma^0 K^+$ , however,  $\pi$ - and  $K$  exchange give rise to contributions of comparable magnitude. This feature becomes very important when we now add the two contributions coherently and consider different choices for the relative sign between the  $\pi$  and  $K$  exchange amplitudes. In one case (indicated by " $K + \pi$ " in Table 2) the  $\pi$  and  $K$  exchange contributions add up constructively for  $pp \rightarrow p\Sigma^0 K^+$  and the resulting total cross section is significantly larger than the individual results. For the other choice (indicated by " $K - \pi$ ") we get a destructive interference between the amplitudes yielding a total cross section that is much smaller. Consequently, in the latter case the cross section ratio is much larger and, as a matter of facts, in rough agreement with the experiment (cf. Table 2).

In this context it is interesting to look at corresponding results for the reaction

$pp \rightarrow n\Sigma^+K^+$ . At the excess energy of 13 MeV the predicted cross sections are 86 (“ $K+\pi$ ”) and 229 nb (“ $K-\pi$ ”), respectively. Thus, the interference pattern is just the opposite as for  $pp \rightarrow p\Sigma^0K^+$ , cf. Table 2. For the “ $K-\pi$ ” case favoured by the experimental  $\sigma_\Lambda/\sigma_{\Sigma^0}$  ratio our calculation yields a cross section for  $pp \rightarrow n\Sigma^+K^+$  that is about 3 times larger than the one for  $pp \rightarrow p\Sigma^0K^+$ . Such a ratio is in fair agreement with data and model calculations at higher energies, see, e.g. Ref. [7]. The other choice, “ $K+\pi$ ”, leads to a  $\sigma_{\Sigma^+}$  that is a factor of about 3 smaller than  $\sigma_{\Sigma^0}$  - a result which is rather difficult to reconcile with the present knowledge about these reactions at higher energies. Obviously it would be very interesting to determine also the ratio  $\sigma_{\Sigma^+}/\sigma_{\Sigma^0}$  close to threshold. It could be measured at, e.g., the COSY facility in Jülich [29].

The results based on the Nijmegen model NSC97f [14] are compiled in Table 3. It is evident that the actual values of the cross sections as well as for the ratios are rather different from those obtained with the Jülich  $YN$  interaction. Most strikingly the FSI (i.e. conversion effects) no longer leads to an enhancement of the cross section ratio in case of  $K$  exchange but to a reduction. Consequently, neither  $K$ - nor  $\pi$  exchange lead to a ratio anywhere near to the experimental value. On a qualitative level, however, the results are still very similar. Again  $K$  exchange is the dominant production mechanism for the reaction  $pp \rightarrow p\Lambda K^+$ , whereas for  $pp \rightarrow p\Sigma^0K^+$   $K$ - as well as  $\pi$  exchange yield contributions of comparable magnitude. Thus, like for the Jülich model, a large cross section ratio  $\sigma_\Lambda/\sigma_{\Sigma^0}$  can only be achieved if there is a destructive interference between the  $K$ - and  $\pi$  exchange in the reaction  $pp \rightarrow p\Sigma^0K^+$  (though such an interference does not occur anymore for the same specific phase between the  $K$ - and  $\pi$  exchange as chosen for the Jülich model, cf. Table 3).

We have also carried out calculations utilizing the other  $YN$  models presented in Ref. [14] (NSC97a-e). The pertinent results exhibit again strong variations in the details. But qualitatively they are similar to the ones discussed above and therefore confirm our findings. Thus we refrain from showing them here explicitly.

Evidently, the results for the cross sections as well as of the ratios depend significantly on the employed FSI. Accordingly, the good agreement of the predictions based on the Jülich  $YN$  model A with the experiment is certainly accidental. But the important message following from our investigation is that only a destructive interference between  $\pi$  and  $K$  exchange can yield fairly large cross section ratios and therefore does offer a possible explanation for the experiment. If the two production mechanisms add up constructively there is little chance of ever coming anywhere close to the experimental value of the ratio, as can be seen from the Tables. We should emphasize, however, that our findings are based on the assumption that  $\pi$  and  $K$  exchange are the dominant

mechanisms for associated strangeness production. This postulate is certainly not unreasonable as demonstrated by the success of earlier investigations on the reaction  $pp \rightarrow p\Lambda K^+$  [7,8,10]. But it is conceivable that other production mechanisms like the direct production or the exchange of heavier mesons, specifically of the vector mesons  $\rho$  and  $K^*$ , play a role as well [9,11]. This, of course, leads to quite a different scenario and it is certainly desirable to carry out investigations in this direction in the future.

In Fig. 3 we show the total cross sections as a function of the excess energy for the “ $K-\pi$ ” case and with the Jülich  $YN$  model as the FSI. It is clear from Table 2 that our model calculations overestimates the absolute values of the empirical cross sections by roughly a factor 4. This is not too surprising because, as already mentioned earlier, effects from the ISI are not taken into account. Therefore, we normalized the results by the factors 0.25 ( $pp \rightarrow p\Lambda K^+$ ) and 0.30 ( $pp \rightarrow p\Sigma^0 K^+$ ), respectively. Then it can be easily seen that the model calculations yield an energy dependence that is in rather nice agreement with the experiment. This suggests that, like in the case of pion production [30,31], the energy dependence of the cross section is primarily influenced by the FSI between the baryons and that effects from other possible FSI’s (in the  $KN$  and/or  $KY$  systems) play a minor role.

In summary, we have studied the reactions  $pp \rightarrow p\Lambda K^+$  and  $pp \rightarrow p\Sigma^0 K^+$  near their thresholds. The strangeness production process is described by the  $\pi$ - and  $K$  exchange mechanisms. Effects from the final state interaction in the hyperon-nucleon system are taken into account rigorously. Our study suggests that the  $\Lambda$  production is dominated by  $K$  exchange whereas  $K$ - as well as  $\pi$  exchange play an important role for the  $\Sigma^0$  case. Furthermore we found that the experimentally observed large cross section ratio  $\sigma_{pp \rightarrow p\Lambda K^+}/\sigma_{pp \rightarrow p\Sigma^0 K^+}$  (at the same excess energy) of around 25 cannot be explained by FSI effects. Rather we conclude from our investigation that a destructive interference between  $\pi$  and  $K$  exchange in the reaction  $pp \rightarrow p\Sigma^0 K^+$  could be the origin of the strong suppression of  $\Sigma^0$  production.

## Acknowledgments

We acknowledge communications with A. Deloff and J.M. Laget concerning their model calculations of the associated strangeness production. C.H. is grateful for the financial support through a Feodor-Lynen Fellowship of the Alexander-von-Humboldt Foundation (DE-FG03-97ER41014). This work was also supported by the INTAS grant no. 96-0597.



## References

- [1] J.T. Balewski et al., Phys. Lett. B **420**, 211 (1998).
- [2] R. Bilger et al., Phys. Lett. B **420**, 217 (1998).
- [3] S. Sewerin et al., Phys. Rev. Lett. **83**, 682 (1999).
- [4] V. Flaminio et al., Compilation of cross sections, CERN-HERA report 79-03 (1979).
- [5] S.E. Vigdor, in *Intermediate Energy Spin Physics*, ed. by F. Rathmann, W.T.H. van Oers, and C. Wilkin, Progress Report 11/1998 (Forschungszentrum Jülich GmbH, Jülich 1998), p. 193.
- [6] J.J. De Swart, Rev. Mod. Phys. **35**, 916 (1963);  
C.B. Dover and A. Gal, Prog. Part. Nucl. Phys. **12**, 171 (1984).
- [7] J.M. Laget, Phys. Lett. B **259**, 24 (1991).
- [8] G.Q. Li and C.M. Ko, Nucl. Phys. **A594**, 439 (1995); G.Q. Li, C.-H. Lee, and G.E. Brown, Nucl. Phys. **A625**, 372 (1997).
- [9] K. Tsushima, A. Sibirtsev, and A.W. Thomas, Phys. Lett. B **390**, 29 (1997);  
K. Tsushima, A. Sibirtsev, A.W. Thomas, and G.Q. Li, Phys. Rev. C **59**, 369 (1999).
- [10] A. Sibirtsev and W. Cassing, nucl-th/9802019.
- [11] N. Kaiser, Eur. Phys. J. A **5**, 105 (1999).
- [12] R. Shyam, Phys. Rev. C **60**, 055213 (1999).
- [13] B. Holzenkamp et al., Nucl. Phys. **A500**, 485 (1989).
- [14] Th.A. Rijken, V.G.J. Stoks, and Y. Yamamoto, Phys. Rev. C **59**, 21 (1999).
- [15] R. Siebert et al., Nucl. Phys. **A567**, 819 (1994).
- [16] D. Cline, R. Laumann, and J. Mapp, Phys. Rev. Lett. **20**, 1452 (1968); T.H. Tan, Phys. Rev. Lett. **23**, 395 (1969).
- [17] A. Kudryavtsev, JETP Lett. **14**, 90 (1971).
- [18] R.H. Dalitz and A. Deloff, Czech. J. Phys. B **32**, 1021 (1982); Aust. J. Phys. **36**, 617 (1983).
- [19] R. Machleidt, K. Holinde and Ch. Elster, Phys. Rep. **149**, 1 (1989).
- [20] A. Reuber, K. Holinde, H.-C. Kim, and J. Speth, Nucl. Phys. **A608**, 243 (1996).
- [21] J. D. Bjorken, S. D. Drell, *Relativistic quantum mechanics*, McGraw-Hill, New York (1964).
- [22] M. Hoffmann et al., Nucl. Phys. **A593**, 341 (1995).

- [23] M. Hoffmann, Jülich report, No. 3238 (1996); M. Hoffmann, in *IKP/COSY Annual Report 1996*, Jül-3365, p. 131.
- [24] R. A. Arndt, L. D. Roper and P. H. Steinberg, Phys. Rev. D **18**, 3278 (1989); C. B. Dover and G. E. Walker, Phys. Rep. **89**, 1 (1989).
- [25] G. Fäldt and C. Wilkin, Z. Phys. **A357**, 241 (1997).
- [26] J.J. Jones et al., Phys. Rev. Lett. **26**, 860 (1971); R.D. Baker et al., Nucl. Phys. **B141**, 29 (1978).
- [27] M. Batinić, A. Švarc, and T.-S. H. Lee, Phys. Scripta **56**, 321 (1997).
- [28] C. Hanhart and K.Nakayama, Phys. Lett. B **454**, 176 (1999).
- [29] COSY-11 collaboration, private communication.
- [30] G.A. Miller and P.U. Sauer, Phys. Rev. C **44**, 1725 (1991).
- [31] H.O. Meyer et al., Nucl. Phys. **A539**, 633 (1992).

Table 1

Vertex parameters used in the present calculation. In case of the Jülich  $YN$  interaction the same values are used as in the model [13]. For the Nijmegen potential only the coupling constants are taken over from Ref. [14].

	Jülich model A			Nijmegen model NSC97f		
<i>Vertex</i>	$g/\sqrt{4\pi}$	$f/\sqrt{4\pi}$	$\Lambda$ [GeV]	$g/\sqrt{4\pi}$	$f/\sqrt{4\pi}$	$\Lambda$ [GeV]
$NN\pi$	3.795	0.282	1.3	3.671	0.273	1.3
$N\Lambda K$	-3.944	-0.268	1.2	-4.925	-0.335	1.3
$N\Sigma K$	0.759	0.0497	2.0	1.501	0.0983	1.3

Table 2

Contributions of different diagrams to the total cross section of the reactions  $pp \rightarrow p\Lambda K^+, p\Sigma^0 K^+$ . The results for  $\Lambda$  ( $\Sigma^0$ ) production are for the excess energy of 13.2 MeV (13.0 MeV). The Jülich  $YN$  model A [13] is employed for the final-state interaction. The indication for the diagrams refers to Fig. 2. In case of “diagonal” only the diagonal channel is included in the intermediate state, i.e. only  $p\Lambda$  for  $\Lambda$  production and  $p\Sigma^0$  and  $n\Sigma^+$  for  $\Sigma^0$  production.

	diagrams	$\sigma_{pp \rightarrow p\Lambda K^+}$ [nb]	$\sigma_{pp \rightarrow p\Sigma^0 K^+}$ [nb]	$\frac{\sigma_{pp \rightarrow p\Lambda K^+}}{\sigma_{pp \rightarrow p\Sigma^0 K^+}}$
$K$	(a)	739	46	16
	“diagonal”	1113	34	33
	(a)-(d)	2426	57	43
$\pi$	(e)	71	77	0.9
	“diagonal”	113	104	1.1
	(e)-(h)	113	105	1.1
” $K + \pi$ ”	all	2471	251	9.9
” $K - \pi$ ”	all	2607	73	36
experiment		$505 \pm 33$	$20.1 \pm 3.0$	$25 \pm 6$

Table 3

Same as in Table 2 employing the Nijmegen  $YN$  model NSC97f [14] for the final-state interaction.

	diagrams	$\sigma_{pp \rightarrow p\Lambda K^+} [nb]$	$\sigma_{pp \rightarrow p\Sigma^0 K^+} [nb]$	$\frac{\sigma_{pp \rightarrow p\Lambda K^+}}{\sigma_{pp \rightarrow p\Sigma^0 K^+}}$
$K$	(a)	1598	116	14
	“diagonal”	1207	109	11
	(a)-(d)	1367	209	6.5
$\pi$	(e)	67	73	0.91
	“diagonal”	63	190	0.33
	(e)-(h)	63	219	0.29
” $K + \pi$ ”	all	1460	432	3.4
” $K - \pi$ ”	all	1400	424	3.3
experiment		$505 \pm 33$	$20.1 \pm 3.0$	$25 \pm 6$

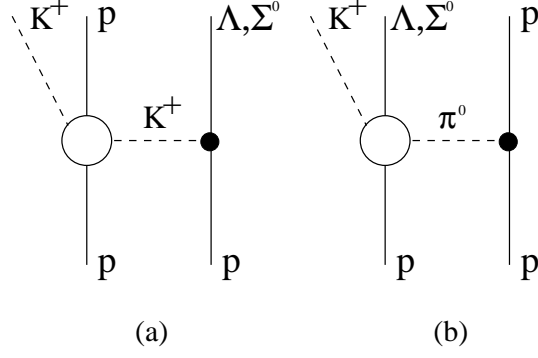


Fig. 1. Mechanisms for the reactions  $pp \rightarrow p\Lambda K^+, p\Sigma^0 K^+$  considered in the present investigation: (a) kaon exchange; (b) pion exchange.

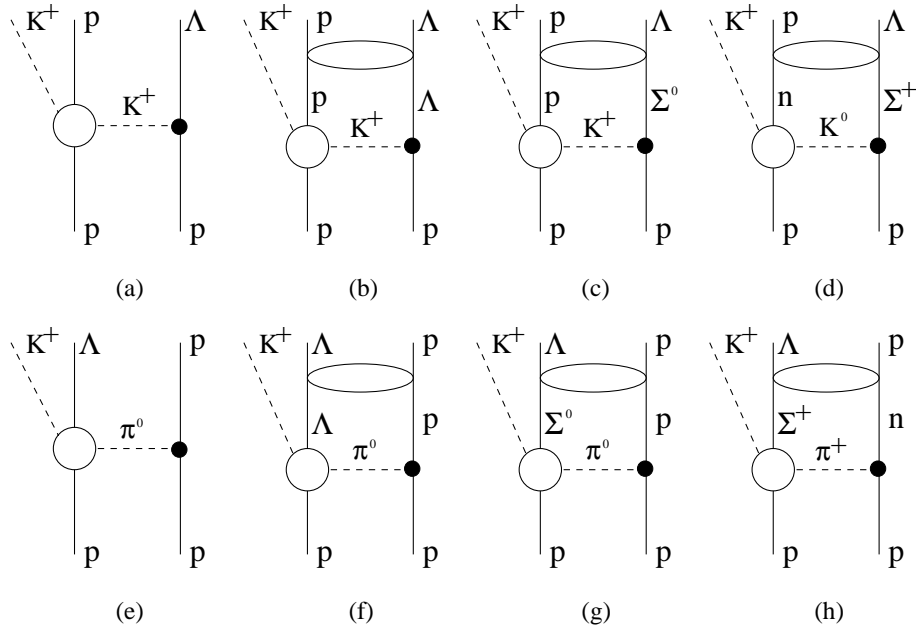


Fig. 2. Contributions to the production amplitude for  $pp \rightarrow pK^+\Lambda$  when the final-state interaction is included, cf. Eq. (1). The open circles and ellipses stand for T-matrices.

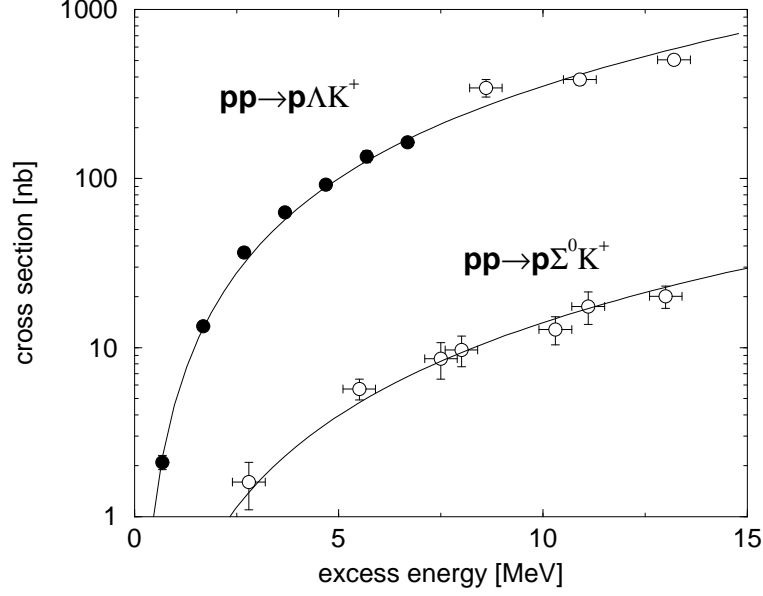


Fig. 3. Total cross sections for the reactions  $pp \rightarrow p\Lambda K^+$  and  $pp \rightarrow p\Sigma^0 K^+$  employing the Jülich  $YN$  model for the FSI. The shown results correspond to the choice “ $K - \pi$ ” for the relative sign, cf. text. The curves for  $pp \rightarrow p\Lambda K^+$  and  $pp \rightarrow p\Sigma^0 K^+$  are normalized by a factor of 0.25 and 0.30, respectively, in order to account for effects of the initial state interaction - as described in the text. The experimental data are from Refs. [1] (filled circles) and [3] (open circles).